

EVALUATION OF TENSILE BEHAVIOR OF ULTRA HIGH PERFORMANCE FIBER REINFORCED CONCRETE WITH UNIAXIAL TENSION TESTS

Di QIAO*¹, Daisuke HONMA*², and Masaro KOJIMA*³

ABSTRACT

The uniaxial tension tests of steel-steel hybrid reinforced ultra-high-performance concrete were carried out to investigate the effects of micro- and macro-fibers on its tensile properties. A dog-bone shaped specimen geometry with a large cross-section size was designed. Although the imperfect test setup introduced bending effects in part of the tests, resulting in an earlier occurrence of first cracking, the tensile strength and strain capacity were found less affected. The test results showed that replacing part of macro-fibers with the micro-fibers can enhance the tensile strength, yet with a cost of ductility. **Keywords:** ultra-high-performance concrete, hybrid fiber system, uniaxial tension test, tensile strength, strain capacity

1. INTRODUCTION

Ultra-high-performance concrete (UHPC) with a compressive strength over 150MPa and significantly fine microstructures is a promising material of achieving the light, slender and durable structures. The steel fibers are generally incorporated to overcome the brittle behavior of the UHPC under tensile loading, known as ultra-high-performance fiber reinforced concrete (UHPRFC). Since a single type of fiber can be useful only in limited ranges of strain and crack growth [1], the hybridization of two or more types of fibers with different sizes and shapes was proposed aiming at better tensile performance than that of mono-fiber reinforced [2, 3]. The idea is that the micro-fibers control the formation and coalescence of fine micro-cracks, while the deformed macro-fibers control the propagation of macro-cracks. Concerning a hybrid system, the uniaxial tension test results reported in [2] showed that the addition of the micro-fibers led to more enhancement in the tensile strength than in the first cracking strength, which is favorable for strain hardening behavior. On the other hand, the results in [3] suggest that the volume fraction of the macro-fibers is crucial to a variety of tensile properties. As the total volumes of the fibers that can be mixed are limited, more knowledge of the effects of micro- and macro-fibers on the tensile behavior of UHPRFC is required for an optimized composition.

This paper presents a study of the tensile response of the UHPRFC with different dosages of hybrid fibers. The uniaxial tension tests using the newly developed dog-bone shaped specimen geometry were carried out, and the effects of the different fibers on the tensile properties were discussed.

2. TEST PROGRAMS

2.1 Materials and Specimen Preparations

The blending micro- and macro-fibers, namely short straight fiber with a length of 13mm and long hooked end fiber with a length of 30mm were added to a UHPC matrix in volume fractions ranging from 2.0% to 3.0%. Table 1 shows the test series. Series 1 had an increasing dosage of macro-fibers with a constant fraction (1.0%) of micro-fibers, while Series 2 replaced part of macro-fibers in Series 1 to increase the volume fraction of micro-fibers to 1.5%. The geometrical and mechanical properties of the steel fibers are shown in Table 2.

Table 1 Test series

Series	Group	Fiber dosage (% in volume)		
		Total	Micro	Macro
1	S1.0H1.0	2.0	1.0	1.0
	S1.0H1.5	2.5	1.0	1.5
	S1.0H2.0	3.0	1.0	2.0
2	S1.5H0.5	2.0	1.5	0.5
	S1.5H1.0	2.5	1.5	1.0
	S1.5H1.5	3.0	1.5	1.5

The composition of the UHPC matrix used for all specimens is shown in Table 3. The water to binder ratio was 0.11. The cement was low heat Portland cement with a high content (50%) of C₂S, low content of C₃A (3%), and a Blaine fineness of 3740cm²/g. The silica fume in the binder had an average diameter of 0.12μm calculated by using its BET surface area of 11.0m²/g, while the average diameter of the fine silica powder used to improve the workability was 0.25μm. The silica sand used in the matrix had an average

*1 Researcher, Structural Materials Group, Takenaka Research & Development Institute, Dr.E., JCI Member

*2 Associate Chief Researcher, Takenaka Research & Development Institute, M.E., JCI Member

*3 Group Leader, Takenaka Research & Development Institute, M.E., JCI Member

Table 2 Properties of high strength steel fibers used in this study

Type	Notation	Density (g/cm ³)	Length (mm)	Diameter (mm)	Aspect ratio	Tensile strength (MPa)	Elastic modulus (GPa)
Micro-fiber	S	7.85	13	0.16	81	>2000	206
Macro-fiber	H	7.85	30	0.38	79	>2610	206

diameter of 0.212mm. A superplasticizer based on the polycarboxylic acid system was adopted to get satisfied fluidity of the UHPC matrix; the average value of the table flow (JIS R 5201 [4]) before adding the fibers was adjusted to about 270mm for avoiding fiber segregation.

Table 3 Composition of UHPC matrix

Type	Proportions by weight	Density (g/cm ³)
Binder	Low heat cement	0.76
	Silica fume	0.12
	Silica fine powder	0.12
	Water	0.11
	Superplasticizer (solid content)	0.0112
Antifoaming agent	0.0003	1.0
Silica sand	0.38	2.60

The mixing was performed using a soil type mixer with a capacity of 30 liters. Half of the binder and silica sand were first dry-mixed for 30 seconds, and then water pre-mixed with the superplasticizer and the

antifoaming agent was added and mixed for two minutes. The adding of the left ingredients was divided into two times. After that, the UHPC mixture was mixed for ten minutes. The micro-fibers were dispersed by hand into the mixture, and then the macro-fibers were added. The mixing was resumed for another seven minutes.

During the specimen preparations, the table flow tests were carried out before and after adding the fibers into the UHPC matrix for each fiber dosage. Both the 100mm long cylindrical specimens with a diameter of 50mm used for the compression tests (three for each test group) and the newly developed dog-bone shaped specimens for the uniaxial tension tests (three for S1.0H2.0 and six for the other groups) were prepared. Although the size of the compression test specimens is considered small in comparison to the length of fibers, which can cause a preferred alignment of fibers along the vertical axis, the influence on compressive strength is marginal [5].

For specimen casting, the UHPC mixture with fibers was placed in two layers; slight vibrations with duration no more than 30 seconds for each layer were applied. After the casting was completed, the specimens were covered with plastic sheets and stored in a curing

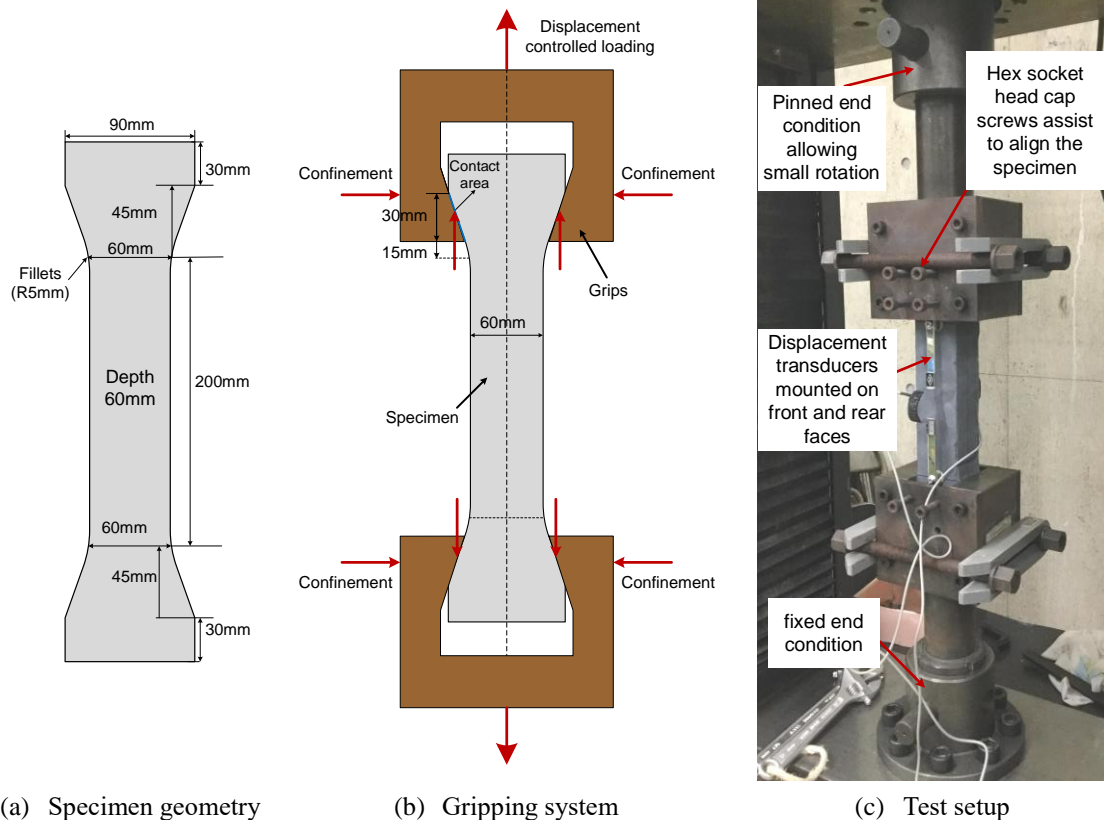
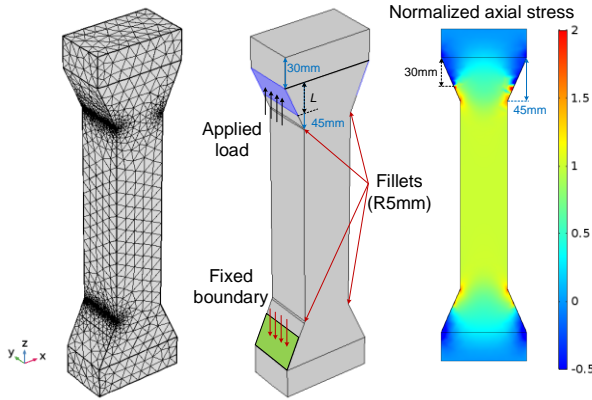
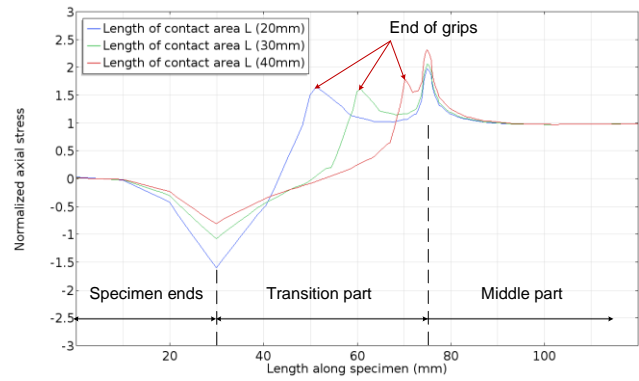


Fig.1 Uniaxial tension test setup used in this study



(a) Modeling details and contours of axial stress



(b) Effect of length of contact area on stress state

Fig.2 Finite element modeling of tensile specimen geometry

room at 20°C with a relative humidity of about 95% for 48h before demolding. The demolded specimens were then cured in a steam chamber under a high temperature of 90°C. The curing temperature was increased at a rate of 15°C per hour up to 90°C and then held at 90°C for 72h. Afterward, the temperature was decreased to 20°C at a rate of 10°C per hour. The mechanical tests proceeded after the steam curing was completed.

2.2 Uniaxial Tension Test Method

Although uniaxial tension tests can directly capture the material tensile behavior including elastic and strain hardening/softening behavior compared with flexural tests that require a back-calculation process, the tension tests are sensitive and difficult to perform. The difficulties lie in several factors, such as a suitable specimen shape to avoid the failure near the grips, correct specimen alignment and proper gripping system to obtain a uniform stress distribution across the specimen cross section [6]. Using the dog-bone shaped specimen with increasing cross sections towards the specimen ends can help to reduce the boundary stress and to avoid failure occurring at the ends generally. JSCE [7] has provided a recommendation using such a specimen shape to perform the uniaxial tension test of HPRCC. The specimen as suggested, however, has a relatively small cross-section (30×30mm²) in the middle part compared with the length of the macro-fibers used in this study. This may cause the fibers aligned to the loading direction and thus yield an overestimation of the tensile performance. Therefore, a new specimen geometry with a larger cross-section is desired.

Fig. 1(a) shows the specimen geometry designed. The size of the constant area in the middle part was increased to 60×60mm², and the length of this part was 200mm to facilitate the observation of multiple cracking behavior. Continuous transitions from the middle part to the specimen ends together with the fillets at the starting points of the transitions were introduced to reduce the effect of stress concentration. The specimen was clamped to the loading machine using the grips with an inner shape like that of the specimen ends (see Fig. 1(b)).

Furthermore, finite element analyses using

commercial software, COMSOL, were carried out to check the stress distribution along the designed geometry, similar to those performed in [6, 8]. The elastic modulus and Poisson's ratio were assumed as 50GPa and 0.2, respectively. Fig. 2(a) shows the unstructured tetrahedral mesh created and a contour plot of the axial stress normalized against the value in the middle part. It was found that the length of the contact area between the specimen transition part and the grip significantly affects the stress state at the starting points of the transition part. As this length reduced, the stress concentration at the starting point of the transition would alleviate as shown in Fig. 2(b). Accordingly, the physical length of the transition part was adjusted for ensuring that failure occurs in the middle part as shown in Fig. 1(b). The tension test results also confirmed that most of the specimens (five out of six specimens at least; all for S1.0H2.0) achieved such a failure.

A universal testing machine with a capacity of 250kN operated in displacement control mode was used to conduct the tension tests. The displacement rate was set as 0.4mm/min, and the boundary conditions of the gripping system were pinned-fixed [9] as shown in Fig. 1(c). Before testing, the installment of the test specimen was carefully performed with the assistance of the hex socket head cap screws (see Fig. 1(c)), and the alignment was checked using a bubble level. Two strain gauge typed displacement transducers with a gauge length of 200mm and a capacity of ±2mm were mounted on the front and rear faces of the specimen, respectively. The averaged value of the measured displacements was used to calculate the strain up to the peak load.

3. TEST RESULTS AND DISCUSSION

3.1 Fresh Properties

Fig. 3 shows the changes in the table flow values after adding the steel fibers to the UHPC mixture. As the total fiber volume fraction increased to 3.0%, the flowability decreased drastically, and mild fiber clumping was observed. The mechanical tests results, however, showed satisfied consistency as presented later. Comparing series 1 and 2, it appears that the

Table 4 Mechanical test results

Series	Group	Compression test		Tension test	
		Compression strength f_c' (MPa)	Elastic modulus E_c (GPa)	Tensile strength σ_{pc} (MPa)	Strain capacity ϵ_{pc} (%)
1	S1.0H1.0	309(3)	52.7(1.1)	12.9(1.5)	0.555(0.141)
	S1.0H1.5	304(10)	54.6(0.4)	14.5(1.4)	0.554(0.148)
	S1.0H2.0	290(6)	54.5(1.1)	14.9(1.2)	0.640(0.092)
2	S1.5H0.5	310(5)	53.4(0.8)	13.1(1.9)	0.377(0.156)
	S1.5H1.0	304(11)	54.2(0.8)	15.7(1.6)	0.509(0.060)
	S1.5H1.5	313(6)	54.1(1.6)	18.3(1.1)	0.615(0.184)

Note: () indicates the standard deviation

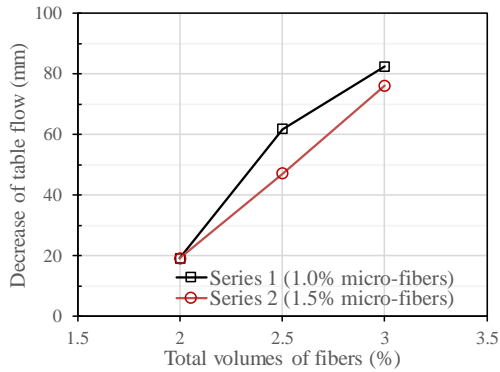
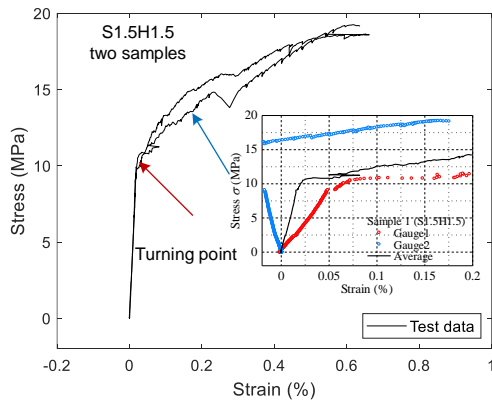


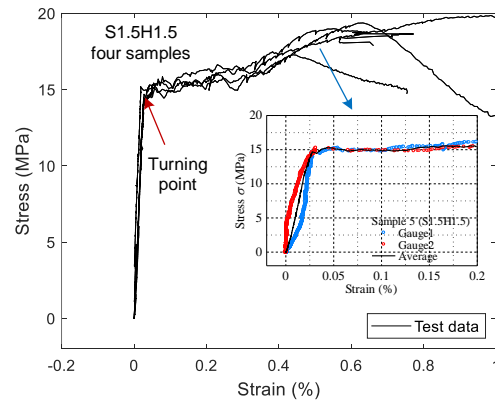
Fig.3 Effect of fiber dosage on table flow



Fig.4 Cracks found in S1.0H2.0 after tension test



(a) Type I influenced by bending



(b) Type II without influence of bending

Fig.5 Typical stress-strain curves in this study

macro-fibers affect the flowability of the UHPFRC mixture more than the micro-fibers even though they have a similar aspect ratio. This is probably due to the interference of the hooked ends with other fibers.

3.2 Compression Test Results

The compression test results are summarized in Table 4. Most of the test groups, which had been steam cured up to 90°C, reached the compressive strength of about 300MPa. As expected, no apparent effect of fiber dosage on the compressive properties was found, since the incorporation of fibers in the UHPC mixture is supposed to improve the ductility of the UHPC under tensile loading.

3.3 Tensile Stress-strain Response

During the tension tests, all specimens showed the strain hardening behavior with the appearance of multiple fine cracks. In the case of S1.0H2.0, more than 50 cracks were found along the 200mm long strain

measuring area as shown in Fig. 4 (cracks are marked in red).

As for the stress-strain curves, two distinctly different curve shapes were observed for a large part of the test groups. Fig. 5 shows an example by the group of S1.5H1.5. The turning point in the curve type I appeared at lower stress than that of type II, indicating an earlier cracking occurrence. Such a difference was caused by the effect of bending, which could be easily discerned by comparing the readings of the two displacement transducers on the front and rear faces. For type I one of the two readings showed negative compressive strains, while for type II the two readings were almost identical. It is considered that the misalignment of the test specimen introduced the undesired bending. The gripping system only allowing the top part to rotate may have exacerbated the problem of misalignment during the testing as well. It requires more work on the test setup to improve the success rate of obtaining a uniform state of stress.

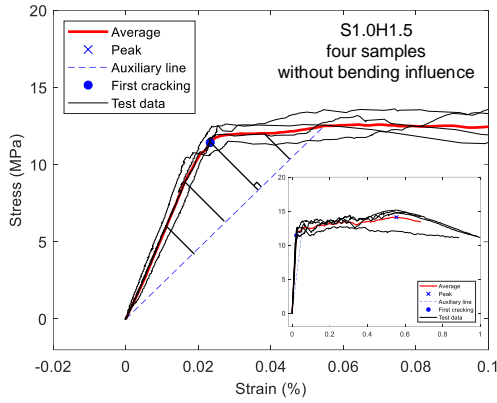


Fig.6 Detect the first cracking point

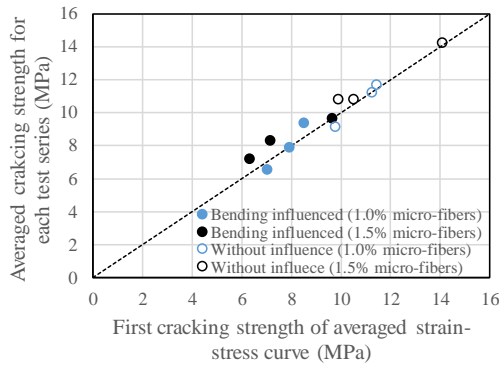
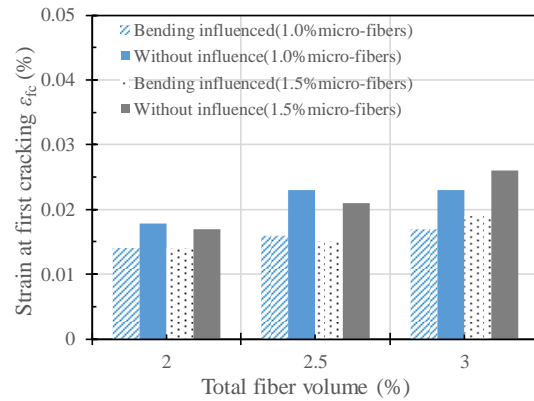
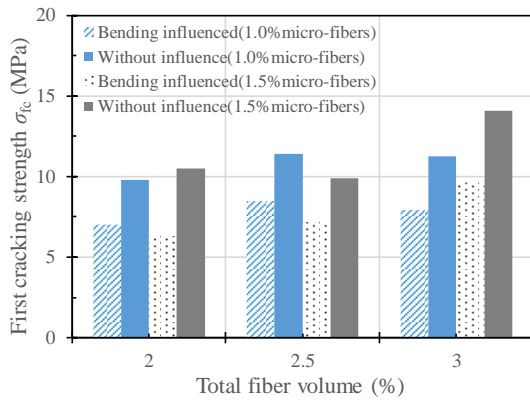
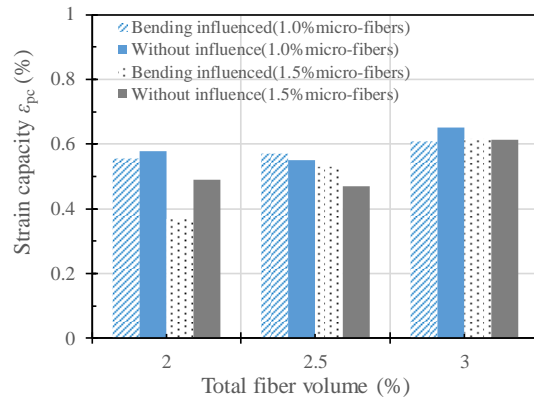
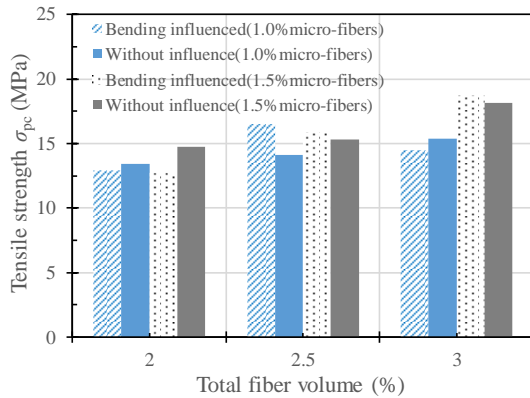


Fig.7 Comparison of methods of detecting first cracking strength



(a) On first cracking



(b) On peak point

Fig.8 Effects of bending on the tensile properties

Detailed information about the tensile properties including the first cracking strength σ_{fc} , the strain at the first cracking ϵ_{fc} , the tensile strength σ_{pc} , and the strain at the peak that is strain capacity ϵ_{pc} was determined for further understanding the effect of bending on these parameters. Fig. 6 illustrates the method of detecting the first cracking point in the stress-strain curves. The averaged curve shown in red was firstly obtained by averaging the stress values of each curve at the same strain levels. The turning point before the peak, which was defined as the first cracking, was then found by searching the longest perpendicular line from the data points to the auxiliary line connecting the zero point and the $0.8\sigma_{pc}$ point (see the dashed line in Fig. 6). A MATLAB script was programmed to perform this task for minimizing the subjectivity automatically. Fig. 7 shows a comparison between the proposed method and the existing one as used in [1, 2], which finds the inflection points of measured strain-stress curves and takes the average. A good agreement can be found.

Fig. 8 shows the effects of bending on the tensile parameters. It appears that although the bending caused significant decreases in the values of σ_{fc} and ϵ_{fc} by about 30%, its influence on the peak point (σ_{pc} and ϵ_{pc}) was comparatively small. This is likely due to the effective bridging of cracks by the steel fibers and the consequent self-adjustment of the top rotating grip. Therefore, the results of the averaged σ_{pc} and ϵ_{pc} considering all the specimens as provided in Table 4 were used to discuss the effects of different fibers on the tensile performance as follows.

3.4 Effects of Micro- and Macro-fibers on Tensile Properties

Fig. 9 and Fig. 10 present the effects of fiber dosage on the tensile strength and the strain capacity, respectively. The increase of the tensile performance is evident as the total fiber volumes are increased. Moreover, for the same total volumes, increasing the proportion of the micro-fibers like Series 2 may lead to an enhancement of the tensile strength, but compromise the strain capacity. As suggested in [2, 3], the developing of tensile stress depends on the degrees of matrix damage resulting from the pullout behavior of the macro-fibers, which involves the deformation of the hooked ends to activate the mechanical bond. The present results showed that replacing part of the macro-fibers with the micro-fibers might be able to mitigate the matrix damage, thus favoring the increased tensile strength. It, however, resulted in a trade-off with the strain capacity as shown by the lower strain values of Series 2 in Fig. 9. Therefore, it is critical to find the optimal combination of the micro- and macro-fibers for improving the tensile performance of UHPFRC in both strength and ductility. It appears that with the UHPC matrix used in this study at least 1.0% macro-fibers are required to obtain the strain capacity of 0.5%.

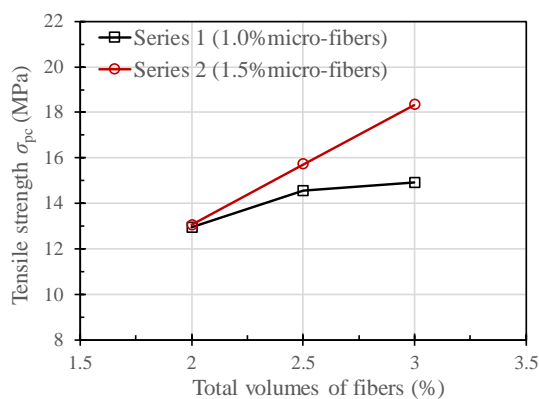


Fig.9 Effects of fiber dosage on tensile strength

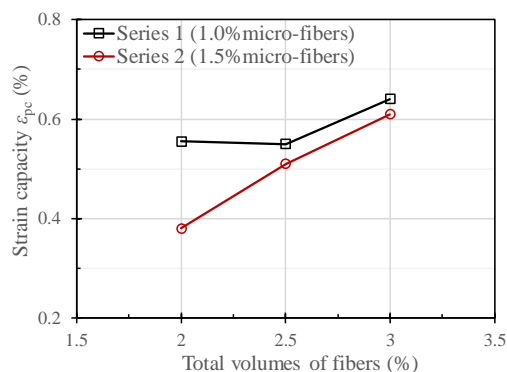


Fig.10 Effects of fiber dosage on strain capacity

4. CONCLUSIONS

This study investigated the effects of blending micro- and macro-fibers on the tensile performance of UHPFRC through the uniaxial tension tests. For this purpose, a dog-bone shaped specimen geometry was developed, which had a larger cross section of

60×60mm² in the middle part. The following conclusions can be derived from this study:

- (1) The designed specimen geometry had a high probability of obtaining failure in the middle part. On the other hand, the current test setup, such as the specimen alignment and the boundary conditions of the gripping system may cause undesired bending during testing. Future work is required to improve the test setup.
- (2) The bending effect resulted in an earlier appearance of the first cracking, while the tensile strength and the strain capacity were affected less.
- (3) The test results showed that increasing the proportion of the micro-fibers in the hybrid system can enhance the tensile strength but at the cost of ductility.
- (4) With the UHPC matrix used in this study, S1.5H1.0 exhibited a competitive performance ($\sigma_{pc} > 15\text{MPa}$ and $\epsilon_{pc} > 0.5\%$) without the problem of fiber clumping.

REFERENCES

- [1] Wille, K., Kim, D. J. and Naaman, A. E., "Strain-hardening UHP-FRC with low fiber contents," *Mater. Struct.*, Vol. 44, 2011, pp. 583-598.
- [2] Park, S. H. et al., "Tensile behavior of ultra high performance hybrid fiber reinforced concrete," *Cem. & Concr. Comp.*, Vol. 34, 2012, pp. 172-184.
- [3] Kwon, S. et al., "Development of ultra-high-performance hybrid fiber-reinforced cement-based composites," *ACI Mater. J.*, Vol. 111(3), 2014, pp. 309-318.
- [4] JIS R 5201, "Physical testing method for cement," JISC, Tokyo, Japan, 2015. (in Japanese)
- [5] Mansur, M. A. et al., "Stress-strain relationship of high-strength fiber concrete in compression," *J. Mater. Civil Eng.*, Vol. 11(1), 1999, pp. 21-29.
- [6] Benson, S. D. P. and Karihaloo, B. L., "CARDIFRC® - Development and mechanical properties. Part III: Uniaxial tensile response and other mechanical properties," *Mag. Concr. Res.*, Vol. 57(8), 2005, pp. 433-443.
- [7] JSCE, "Recommendations for design and construction of HPRCC with multiple fine cracks," 2008.
- [8] Graybeal, B. A. and Baby, F., "Development of direct tension test method for ultra-high-performance fiber-reinforced concrete," *ACI Mater. J.*, Vol. 110(2), 2013, pp. 177-186.
- [9] Naaman, A. E., Fischer, G. and Krstulovic-Opara, N., "Measurement of tensile properties of fiber reinforced concrete: draft submitted to ACI Committee 544," Fifth International RILEM Workshop on High Performance Fiber Reinforced Cement Composites (HPFRCC5), Mainz, Germany, 2007, pp. 3-12.